Effect of smoothing by spectral dispersion on flow induced laser beam deflection: The random phase modulation scheme

Harvey A. Rose and Sandip Ghosal
Los Alamos National Laboratory, Los Alamos, New Mexico 87545

(Received 11 September 1997; accepted 4 December 1997)

Analytical results are presented for the effect of random phase modulated smoothing by spectral dispersion on flow induced laser beam deflection. It is shown that in the limit of a large number of color cycles, N_{cc}, the effect is identical to that of the induced spatial incoherence method of temporal smoothing. For small N_{cc}, the beam deflection rate may be significantly larger in the direction perpendicular to the dispersion, than in the parallel direction. © *1998 American Institute of Physics.* [S1070-664X(98)02503-8]

I. INTRODUCTION

Accurate pointing of high power laser beams is required to achieve high gain implosions of capsules in inertial confinement fusion.[1] To the extent that laser ray trajectories are calculated on the basis of macroscopic refractive effects alone, this pointing may be in error, as has been observed in various experiments.[2–5] This nonclassical beam deflection has been attributed[6,7] to the combined effect of flow transverse to the laser beam and diffraction by microscopic density fluctuations induced by laser speckles or ''hot spots.''

Previous closed form analytical results for beam deflection by flow have been obtained[8,9] for a model which allows only spatial incoherence as induced by a random phase plate[10] (RPP), and for a model of induced spatial incoherence[11] (ISI) where there is also temporal smoothing. The key simplification of these models is the assumption that the laser intensity pattern is that obtained in a quiescent plasma, which requires at the least that self-focusing be ignorable, as discussed in Ref. 9.

In this paper the first analytic theory of beam deflection by flow is presented for the case of a laser beam which is spatially smoothed by a RPP and temporally smoothed by the random phase modulation variety of smoothing by spectral dispersion[12] (SSD). It is shown that in the limit of a large number of color cycles, N_{cc}, the effect is identical to that of the induced spatial incoherence method of temporal smoothing. For small N_{cc}, and general flow direction, the beam deflection rate may be significantly larger in the direction perpendicular to the dispersion, than in the parallel direction. Since by symmetry considerations, one expects little azimuthal plasma flow in a hohlraum, this result implies that the dispersive direction for each beam be chosen in the radial direction to minimize nonclassical beam deflection.

For either very small acoustic wave damping, or for a convenient choice of electric field temporal correlation function, the determination of beam deflection is reduced to the evaluation of a two dimensional integral over a finite domain of fourier space. After introducing the SSD model, the intensity correlation function is determined in Sec. III. Using the linearized hydrodynamic approximation, the basic expression for beam deflection is presented in Sec. IV and in the large bandwidth limit specific scaling and numerical results are obtained in Sec. V.

II. THE SSD MODEL

A simplified model of SSD is obtained by assigning a phase, $\phi(\mathbf{k},t)$, to each Fourier mode of the laser light electric field, $\mathbf{E}$ (in a particular plane $z=$constant of the optic focal region), which is the sum of two parts: a static component owing to the RPP, $\phi(\mathbf{k})$, which for each $\mathbf{k}=(k_x,k_y)$, is a statistically independent random variable, such that

$$\langle \exp i[\phi(\mathbf{k})-\phi(\mathbf{k}')]\rangle_{\phi}=\delta_{\mathbf{kk}'}, \tag{1}$$

where $\langle\ \rangle_{\phi}$ means ensemble average with respect to the RPP phases; and an independent, time varying part owing to spectral dispersion in the ''x'' direction, $\theta(\beta k_x - t)$,

$$\mathbf{E}=\hat{\mathbf{e}}\ \mathrm{Re}\{\epsilon(\mathbf{x},t)\exp(-i\omega_0 t)\}, \tag{2}$$

$$\epsilon(\mathbf{x},t)=\sum_{\mathbf{k}}|\hat{\epsilon}(\mathbf{k})|\exp i[\mathbf{k}\cdot\mathbf{x}+\phi(\mathbf{k},t)], \tag{3}$$

$$\phi(\mathbf{k},t)=\phi(\mathbf{k})+\theta(\beta k_x-t). \tag{4}$$

$\hat{\mathbf{e}}$ is a unit vector in the $x-y$ plane, $\mathbf{x}=(x,y)$, and ω_0 is the laser angular frequency. In the top hat model of intensity distribution across the RPP, $|\hat{\epsilon}|$ is a constant for $|\mathbf{k}| \leqslant k_0/(2F)$, and vanishes otherwise, where k_0 is the laser wave number and F is the optic ''F'' number. $\beta=sf/k_0$, where s is the temporal ''skew'' of the diffraction grating and f is the optic focal length.

The functional form of θ is often chosen as $\theta(t) \propto \sin(\nu t)$, i.e., frequency modulation (FM), as in Ref. 12, but in this paper it will be chosen to be random, in a sense made precise below, to produce a random phase modulation[13–16] (RPM) variant of SSD, which is amenable to analytical analysis.

III. INTENSITY CORRELATIONS

The beam deflection rate may be written as[6]

$$\frac{d\hat{\mathbf{k}}_0}{dz}=-\frac{1}{2n_c}\frac{\int d\mathbf{x}U\nabla n}{\int d\mathbf{x}U}, \tag{5}$$

 © 1998 American Institute of Physics

Downloaded 10 Mar 2009 to 129.105.69.71. Redistribution subject to AIP license or copyright; see http://pop.aip.org/pop/copyright.jsp

where the ponderomotive potential $U\propto|\epsilon|^2$, $\hat{\mathbf{k}}_0$ is a unit vector in the laser beam direction, and n_c is the critical plasma density. In hydrodynamics linearized about a spatially uniform state, (see Sec. IV), ∇n is proportional to the superposition of U at earlier times and other spatial locations. Since the fluctuations of ϵ are spatially homogeneous, the spatial integrals may be replaced by ensemble average, denoted by $\langle\ \rangle$, provided that the size of the domain is large compared to the correlation length of the fluctuations in $|\epsilon|^2$,

$$\frac{d\hat{\mathbf{k}}_0}{dz}=-\frac{1}{2n_c}\frac{\langle U\nabla n\rangle}{\langle U\rangle}=-\frac{1}{2n_c}\frac{\langle \delta U\nabla \delta n\rangle}{\langle U\rangle}, \tag{6}$$

where $\delta U(\mathbf{x},t)=U(\mathbf{x},t)-\langle U\rangle$ and $\delta n(\mathbf{x},t)=n(\mathbf{x},t)-\langle n\rangle$. The numerator may be expressed in terms of the two point autocorrelation function of $|\epsilon|^2$ which will now be evaluated.

It follows from Eqs. (1), (3), and (4) that the fluctuations of ϵ are spatially homogeneous with

$$\langle \epsilon(\mathbf{x},t)\epsilon^*(0,t')\rangle_\phi=\sum_{\mathbf{k}} |\hat{\epsilon}(\mathbf{k})|^2 \exp i[\mathbf{k}\cdot\mathbf{x}+\theta(\beta k_x-t)-\theta(\beta k_x-t')]. \tag{7}$$

Let the fluctuations of θ, as determined by RPM, be temporally homogeneous with

$$\langle \exp i[\theta(t)-\theta(t')]\rangle_\theta=G(t-t')=G^*(t'-t), \tag{8}$$

where $\langle\ \rangle_\theta$ means average with respect to the random process of the RPM. Now let $\langle\ \rangle$ denote the average over both phases. It follows from Eqs. (7) and (8) that

$$\langle \epsilon(\mathbf{x},t)\epsilon^*(0,t')\rangle=G^*(t-t')\sum_{\mathbf{k}} |\hat{\epsilon}(\mathbf{k},t)|^2 \exp i(\mathbf{k}\cdot\mathbf{x}) \equiv B(\mathbf{x})G^*(t-t'). \tag{9}$$

Now evaluate the normalized ponderomotive autocorrelation function,

$$C(\mathbf{x}-\mathbf{x}',t-t')=\langle \delta U(\mathbf{x},t)\,\delta U(\mathbf{x}',t')\rangle/\langle U\rangle^2. \tag{10}$$

It follows from Eqs. (1), (3), and (4) for arbitrary space time points, 1, 2, 3, and 4, that

$$\langle \epsilon(1)\epsilon^*(2)\epsilon(3)\epsilon^*(4)\rangle_\phi=\langle \epsilon(1)\epsilon^*(2)\rangle_\phi\langle \epsilon(3)\epsilon^*(4)\rangle_\phi+\langle \epsilon(1)\epsilon^*(4)\rangle_\phi\langle \epsilon(3)\epsilon^*(2)\rangle_\phi, \tag{11}$$

in the limit when the number of Fourier modes with $|\mathbf{k}|\leqslant k_0/(2F)$ is large[17] and therefore Eqs. (10) and (11) imply that

$$\langle \delta U(\mathbf{x},t)\,\delta U(0,t')\rangle_\phi\propto|\langle \epsilon(\mathbf{x},t)\epsilon(0,t')\rangle_\phi|^2. \tag{12}$$

Equation (7) then implies

$$C(\mathbf{x},t-t')\propto\sum_{\mathbf{k}}\sum_{\mathbf{p}} |\hat{\epsilon}(\mathbf{k})|^2|\hat{\epsilon}(\mathbf{p})|^2\mathbf{e}^{i(\mathbf{k}-\mathbf{p})\mathbf{x}} \times\langle \exp i[\theta(\beta k_x-t)-\theta(\beta k_x-t')-\theta(\beta p_x-t)+\theta(\beta p_x-t')]\rangle_\theta. \tag{13}$$

Since the fluctuations of θ are assumed homogeneous, the $\langle\ \rangle_\theta$ factor only depends on $t-t'$, and therefore only upon k_x-p_x. Equation (13) may therefore be re-expressed as

$$C(\mathbf{x},t)=\sum_{\mathbf{q}} \hat{C}_0(\mathbf{q})\mathbf{e}^{i\mathbf{q}\cdot\mathbf{x}}f(q_x,t), \tag{14}$$

with

$$\hat{C}_0(\mathbf{q})=\sum_{\mathbf{k}-\mathbf{p}=\mathbf{q}} |\hat{\epsilon}(\mathbf{k})|^2|\hat{\epsilon}(\mathbf{p})|^2 \Bigg/ \left(\sum_{\mathbf{k}} |\hat{\epsilon}(\mathbf{k})|^2\right)^2, \tag{15}$$

and

$$f(q_x,t)=\langle \exp i[\theta(\beta q_x-t)-\theta(-t)+\theta(0)-\theta(\beta q_x)]\rangle_\theta. \tag{16}$$

Note that the function f has the value unity for $t=0$, and therefore Eqs. (9), (14), and (15) imply $C(\mathbf{x},0)\equiv C_0(\mathbf{x})=|B(\mathbf{x})|^2/|B(0)|^2$, and in particular, $C(0,0)=1$.

A remarkable property of the function f is that it does not decay to zero in the limit of large time separations, even if G does. This can be shown by noting that in this limit the first two terms in the bracket of Eq. (16) are independent of the second two so that

$$f(q_x,t)\underset{t\to\infty}{\to}\langle \exp i[\theta(\beta q_x-t)-\theta(-t)]\rangle_\theta \times\langle \exp i[\theta(0)-\theta(\beta q_x)]\rangle_\theta=|G(\beta q_x)|^2. \tag{17}$$

This is a manifestation of the non-Gaussian fluctuations of ϵ, considered as a random variable whose fluctuations arise both from the RPP and the RPM-SSD. If ϵ were Gaussian with respect to averages over both phases, then it would follow that $\langle \delta U(\mathbf{x},t)\,\delta U(0)\rangle\sim|\langle \epsilon(\mathbf{x},t)\epsilon(0)\rangle|^2=|B(\mathbf{x})G(t)|^2$, which is incorrect, e.g., correlations are predicted to decay to zero at a rate which is independent of the wave number of the fluctuation. Only the fluctuations in ϵ owing to the RPP phases, for given SSD phase θ, are Gaussian.

For finite time separations, f may be related to integral properties of G if it is assumed that the random process, u, defined by $d\theta/dt\equiv u$, is stationary and Gaussian with $\langle u\rangle=0$. Let $\langle u(t)u(t')\rangle=\Phi(t-t')$. The following well known basic result,

$$\left\langle \exp i\int_{-\infty}^{\infty}\eta(r)u(r)dr\right\rangle =\exp\left[-\frac{1}{2}\int_{-\infty}^{\infty}\int_{-\infty}^{\infty}\eta(r)\Phi(r-r')\,\eta(r')drdr'\right], \tag{18}$$

allows for the evaluation of expectation values of the form given in Eq. (16). As an example, if

$$\Phi(t)=\gamma^2 \exp(-\nu|t|), \tag{19}$$

then

Downloaded 10 Mar 2009 to 129.105.69.71. Redistribution subject to AIP license or copyright; see http://pop.aip.org/pop/copyright.jsp

$$G(t)=\langle \exp i[\theta(t)-\theta(0)]\rangle$$
$$=\exp\left[-\frac{\gamma^2}{\nu^2}\left(\nu|t|-1+e^{-\nu|t|}\right)\right], \quad (20)$$

which follows from Eq. (18) with $\eta(r)=1$ for $0<r<t$, and 0 otherwise. If $\gamma/\nu \gg 1$, then G, which is a monotonic decreasing function of $|t|$, may decay to a small value while $\nu|t|\ll 1$, $G(t)\approx \exp(-\gamma^2 t^2/2)$. This is the regime where the ''bandwidth'' of the electric field amplitude, ϵ, is large compared to the bandwidth of the phase, θ.

To evaluate Eq. (16) note that

$$\theta(\beta q_x-t)-\theta(\beta q_x)=\int_{\beta q_x}^{\beta q_x-1} u(r)dr$$
$$\equiv \int_{-\infty}^{\infty}\eta_1(r)u(r)dr,$$

and

$$\theta(0)-\theta(-t)=\int_{-t}^{0}u(r)dr \equiv \int_{-\infty}^{\infty}\eta_2(r)u(r)dr.$$

Set $\eta=\eta_1+\eta_2$ in Eq. (18) to obtain

$$f(q_x,t)=H(\nu\beta|q_x|,\nu|t|,\gamma/\nu), \quad (21)$$

with

$$-\frac{1}{2\mu^2}\log H(\kappa,\tau,\mu)=|\tau|-1+e^{-|\tau|}$$
$$-\left[\frac{1}{2}e^{-|\kappa|}(e^{|\tau|}+e^{-|\tau|}-2)\right] \quad \text{if } |\tau|\leqslant|\kappa|$$
$$-\left[|\tau|-|\kappa|+\frac{1}{2}e^{-(|\tau|-\kappa|)}+\frac{1}{2}e^{-|\kappa|}(e^{-|\tau|}-2)\right] \quad \text{if } |\tau|>|\kappa|. \quad (22)$$

It can be shown that f is a monotonic decreasing function of t and q_x.

A. The large bandwidth limit

Some limits of this function are of particular interest. For $\nu|t|\ll 1$ and $t<\beta|q_x|$

$$f(q_x,t)\approx \exp[-\gamma^2 t^2(1-e^{-\nu\beta|q_x|})]. \quad (23)$$

In order that f decay to a small value before $t<\beta|q_x|$ is violated, it is necessary that

$$\gamma\beta|q_x|=\frac{\gamma}{\nu}\,\nu\beta|q_x|=\frac{\gamma}{\nu}\,N_{cc}F|q_x|/k_0\gg 1, \quad (24)$$

where $N_{cc}\equiv \nu\beta k_0/F$ is the number of ''color cycles''—the number of independent SSD phases across the RPP because from Eq. (4), $\beta k_0/F$ is the time it takes the SSD phase to be swept across the entire phase plate and $1/\nu$ is the phase correlation time. Since $q_x=O(k_0/F)$, this inequality is essentially satisfied if

$$N_{cc}\gamma/\nu \gg 1. \quad (25)$$

In order that f decay to a small value before $\nu|t|\ll 1$ is violated, it is also required that

$$\gamma/\nu\gg 1. \quad (26)$$

If Eqs. (25) and (26) are satisfied, this will be called the large bandwidth limit of RPM-SSD. Note that large bandwidth refers to large bandwidth of the electric field, not the phase of the electric field, as Eq. (26) implies that the bandwidth of the electric field is large compared to that of the phase. Since the minimal implementation of SSD is usually envisioned as having at least one color cycle, Eq. (25) is redundant, given Eq. (26).

B. The ISI limit

If in place of Eq. (25), $N_{cc}\gg 1$ is satisfied, then for most modes

$$\nu\beta|q_x|\gg 1, \quad (27)$$

$f(q_x,t)\approx G^2(t)$, and $C(\mathbf{x},t)$ factors into a function of space times a function of time, just as in the case of ISI for which the beam deflection analysis has been done.[9] If in addition, Eq. (26) is satisfied then $G^2(t)\approx \exp(-\gamma^2 t^2)$.

IV. LINEARIZED HYDRODYNAMIC APPROXIMATION

In our previous study of beam deflection in the RPP[8] case, it was found that for small enough values of the average laser intensity, predictions of the local[18] beam deflection rate based on linearized hydrodynamics were in excellent agreement with those obtained from nonlinear hydrodynamics.[6] Near Mach number unity the differences were the largest, and for strongly damped acoustic waves, with dimensionless Landau damping coefficient, ν_{ia}, of order 0.1, even these differences were small provided that $|\langle\delta n\rangle|/n_0<0.05$, where n_0 is the background density and $|\langle\delta n\rangle|$ is the magnitude of the ponderomotive density response based on the average ponderomotive potential in a quiescent (nonflowing) plasma. In practical units $|\langle\delta n\rangle|/n_0 \approx 0.90\times 10^{-13}(\lambda_0/\mu\mathrm{m})^2(\mathrm{cm}^2\langle I\rangle/\mathrm{W})(\mathrm{eV}/T_e)$, where T_e is the electron temperature, λ_0 is the laser wavelength and $\langle I\rangle$ the average laser intensity.[19] We provisionally assume that the domain of validity of the linear hydro response for the time dependent intensity fluctuations characteristic of RPM-SSD is at least as great as in the RPP case.

For convenience, we choose to represent the linear hydro response of the density fluctuation in the following form

$$\frac{\delta n(\mathbf{x},t)}{n_0}=-\frac{|\langle\delta n\rangle|}{n_0}\int L(\mathbf{x}-\mathbf{x}',t-t')\times\frac{U(\mathbf{x}',t')}{\langle U\rangle}\,d\mathbf{x}'dt', \quad (28)$$

L is simply represented in Fourier space,

$$\hat{L}^{-1}(\mathbf{k},\omega)=1-\left(\frac{\omega-\mathbf{k}\cdot\mathbf{v}_0}{c_s k}\right)^2-2i\nu_{ia}\left(\frac{\omega-\mathbf{k}\cdot\mathbf{v}_0}{c_s k}\right), \quad (29)$$

where c_s is the ion acoustic speed and the transform convention is

Downloaded 10 Mar 2009 to 129.105.69.71. Redistribution subject to AIP license or copyright; see http://pop.aip.org/pop/copyright.jsp

$$\hat{\psi}(\mathbf{k},\omega)=\int\int \psi(\mathbf{x},t)\exp - i(\mathbf{k}\cdot\mathbf{x}-\omega t)d\mathbf{x}dt.$$

$\mathbf{v}_0$ is the projection in the (x,y) plane of the spatially uniform background plasma flow in the frame of reference where the laser electric field is given by Eqs. (2)–(4).

Equations (6), (10), and (28) imply[20]

$$\frac{d\hat{\mathbf{k}}_0}{dz}=\frac{n_0}{2n_c}\frac{|\langle\delta n\rangle|}{n_0}\int C(\mathbf{x},t)\nabla L(\mathbf{x},t)d\mathbf{x}dt, \tag{30}$$

or in Fourier space,

$$\frac{d\hat{\mathbf{k}}_0}{dz}=\frac{n_0}{2n_c}\frac{|\langle\delta n\rangle|}{n_0}\int \mathbf{k}\hat{C}(\mathbf{k},\omega)i\hat{L}(\mathbf{k},\omega)\frac{d\mathbf{k}}{(2\pi)^2}\frac{d\omega}{(2\pi)}, \tag{31}$$

with $\hat{C}(\mathbf{k},\omega)=\hat{C}_0(\mathbf{k})\hat{f}(k_x,\omega)$, and in the limit where Fourier sums are replaced by integrals it follows from Eqs. (14) and (15) that $\hat{C}$ vanishes for $\kappa=Fk/k_0>1$, otherwise

$$\frac{\hat{C}_0(\mathbf{k})}{(2\pi)^2}=\frac{1}{\pi[k_0/(2F)]^2}\left(1-\frac{2}{\pi}\sin^{-1}\kappa-\frac{2}{\pi}\kappa\sqrt{1-\kappa^2}\right)$$
$$\equiv(F/k_0)^2\hat{c}(\kappa). \tag{32}$$

Note that $\hat{c}$ is well approximated by a linear function, $\hat{c}\approx(0.948-1.04\kappa)4/\pi$ for $0\leqslant\kappa\leqslant 0.948/1.04\approx 0.912$, otherwise zero.

V. BEAM DEFLECTION IN THE LARGE BANDWIDTH LIMIT

In the large bandwidth limit, it follows from Eq. (23) that

$$\hat{f}(k_x,\omega)=\frac{\sqrt{\pi}}{\gamma(k_x)}\exp\left[-\frac{\omega^2}{4\gamma^2(k_x)}\right], \tag{33}$$

$$\gamma(k_x)=\gamma\sqrt{1-\exp(-\nu\beta|k_x|)}=\gamma\sqrt{1-\exp(-N_{cc}|\kappa_x|)}.$$

Equations (29), and (31)–(33) and a change of the variables of integration from k to κ and ω to $\Omega=\omega/\gamma(k_x)$ imply that

$$\frac{F}{k_0}\frac{d\hat{\mathbf{k}}_0}{dz}=\mathbf{D}(\mathbf{M},\nu_{ia},g,N_{cc}), \tag{34}$$

where $g\equiv k_0c_s/(F\gamma)$, $\mathbf{M}=\mathbf{v}_0/c_s$, and

$$\mathbf{D}(\mathbf{M},\nu_{ia},g,N_{cc})$$
$$=\frac{n_0}{4\pi n_c}\frac{|\langle\delta n\rangle|}{n_0}\int\sqrt{\pi}e^{-\Omega^2/4}\frac{i\boldsymbol{\kappa}\hat{c}(\kappa)}{1-u^2-2i\nu_{ia}u}\,d\boldsymbol{\kappa}d\Omega, \tag{35}$$

with the argument u in the integrand of Eq. (35) given by

$$u=\frac{\Omega}{g\kappa}\sqrt{1-\exp(-N_{cc}|\kappa_x|)}-\frac{\boldsymbol{\kappa}}{\kappa}\cdot\mathbf{M}. \tag{36}$$

We will have occasion below to regard Ω as a function of u, as given implicitly by Eq. (36). Recall that $\hat{c}$ is defined in Eq. (32). The parameter g may be thought of as the ratio of the electric field correlation time to the speckle width ion acoustic transit time.

It follows from Eqs. (35) and (36) that $\mathbf{D}(-\mathbf{M},.)=-\mathbf{D}(\mathbf{M},.)$, $D_x(M_x,-M_y,.)=D_x(M_x,M_y,.)$ and $D_y(M_x,-M_y,.)=-D_y(M_x,M_y,.)$.

A. The small damping limit

The width of the hydro resonance in Eq. (35), is $du=\nu_{ia}$, or $d\Omega=g\kappa\nu_{ia}/\sqrt{1-\exp(-N_{cc}|\kappa_x|)}$. If $g\nu_{ia}<1$, $d\Omega$ is larger than unity only for small $|\kappa_x|$, $|\kappa_x|=F|k_x|/k_0<(g\nu_{ia})^2/N_{cc}$. Since a minimal requirement for SSD is usually considered to be $N_{cc}\geqslant O(1)$, so long as *the small damping limit*

$$(g\nu_{ia})^2\ll 1 \tag{37}$$

obtains, the hydrodynamic resonance is narrower than that of the ponderomotive fluctuations [the $\exp(-\Omega^2/4)$ term] for most modes. If furthermore $\nu_{ia}\ll 1$, the well known result

$$\frac{1}{1-u^2-2i\epsilon u}\xrightarrow[\epsilon\to 0]{}\frac{i\pi}{2}[\delta(u-1)-\delta(u+1)]$$

allows for the simple evaluation of the Ω integration in Eq. (35) to obtain

$$\mathbf{D}(\mathbf{M},0,g,N_{cc})$$
$$=\frac{n_0}{8n_c}\frac{|\langle\delta n\rangle|}{n_0}g\int\frac{\kappa\boldsymbol{\kappa}\hat{c}(\kappa)}{\sqrt{1-\exp(-N_{cc}|\kappa_x|)}}[\hat{f}]_{\mp}d^2\kappa, \tag{38}$$

with

$$\frac{1}{\sqrt{\pi}}[\hat{f}]_{\mp}=\exp\left[-\frac{\Omega^2(u=-1)}{4}\right]-\exp\left[-\frac{\Omega^2(u=+1)}{4}\right]. \tag{39}$$

Although the y component of the integrand does not remain finite as $|\kappa_x|\to 0$ since

$$\frac{1}{\sqrt{1-\exp(-N_{cc}|\kappa_x|)}}[\hat{f}]_{\mp}\xrightarrow[N_{cc}|\kappa_x|\to 0]{}\frac{1}{\sqrt{N_{cc}|\kappa_x|}}$$

it remains integrable.

Some particular examples are now considered based upon the numerical evaluation of Eq. (38). In Fig. 1, the x

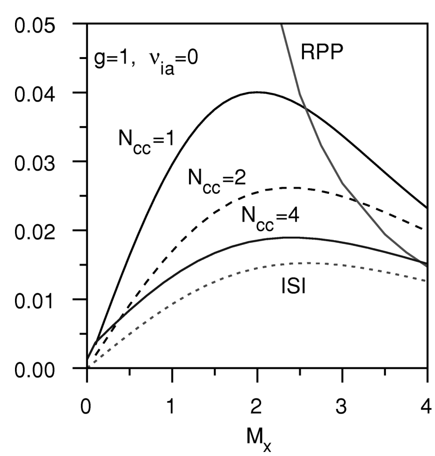

FIG. 1. Normalized deflection rate in the x direction for the case of small Landau damping, with $g=1$ and $M_y=0$.

Downloaded 10 Mar 2009 to 129.105.69.71. Redistribution subject to AIP license or copyright; see http://pop.aip.org/pop/copyright.jsp

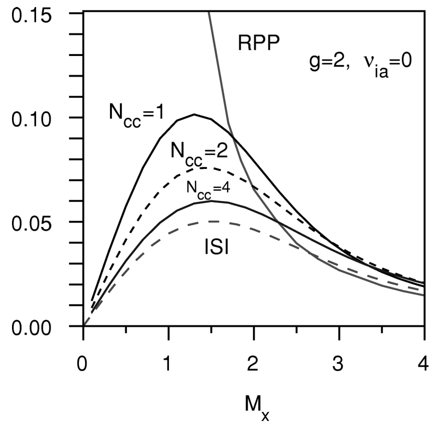

FIG. 2. The $g=2$ variant of Fig. 1.

component of the normalized deflection rate, $n_c\mathbf{D}(\mathbf{M},0,g,N_{cc})/|\langle\delta n\rangle|$ is shown for $g=1$ and $M_y=0$ as a function of M_x and N_{cc}. The curve labeled ''RPP'' is the rate for the case of beam smoothing by an RPP alone, as presented[21] in Ref. 8, and the curve labeled ISI is obtained by replacing the $\sqrt{1-\exp(-N_{cc}|\kappa_x|)}$ factors in Eqs. (33) and (38) by unity, so that the intensity correlations factor into the product of a function of space and a function of time, as discussed in Sec. III B. Similar ISI results have been presented in Ref. 9. Note that the RPM-SSD rate exceeds the ISI rate, which is approached from above for moderate values of N_{cc}. If $M_x<1$, the RPP deflection vanishes for zero acoustic damping and for these Mach numbers the effect of temporal beam smoothing is to increase the deflection rate, as noted previously.[9] The results shown in Fig. 2 are as in Fig. 1, except that $g=2$. In Fig. 3 contours of the magnitude of the normalized deflection rate are shown as a function of $\mathbf{M}$ for $g=1$ and $N_{cc}=1$. For this case $\mathbf{D}$ is approximately parallel to $\mathbf{M}$. The anisotropy of this figure, with the deflection rate peaking along the y axis, the direction perpendicular to the optic dispersive direction, the x axis, may be explained by noting that the rate in the x direction involves an x derivative, as shown in Eq. (30), which is dominated by more rapidly decaying intensity fluctuations, as shown in Eq. (33) for large $|k_x|$, while the rate in the y direction weights larger $|k_y|$ fluctuations, but $|k_x|$ may be small, and the associated

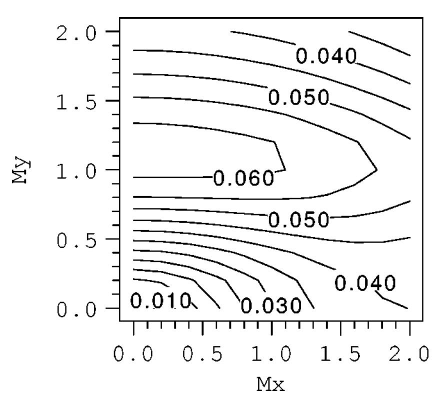

FIG. 3. Contours of the magnitude of the normalized deflection rate are shown as a function of $\mathbf{M}$ for $g=1$ and $N_{cc}=1$ and small Landau damping.

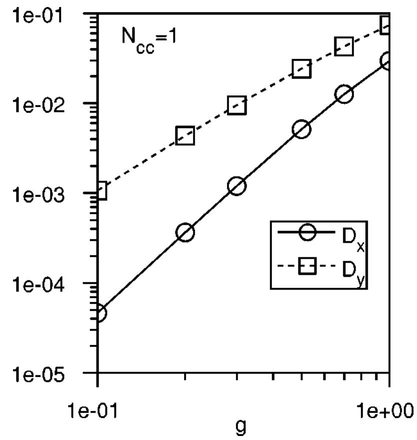

FIG. 4. Normalized x and y deflection rates in the case of small Landau damping, with $N_{cc}=1$, with D_x evaluated for $M_y=0$ and $M_x=1.0$, and D_y evaluated for $M_x=0$ and $M_y=1.0$.

intensity fluctuations are more slowly varying, leading to larger deflection rates. For small g simple scaling estimates presented in the next paragraph show that $D_x/D_y\sim g$. For larger values of N_{cc}, the ISI regime is approached and the contours become nearly circular.

To determine the scaling of $\mathbf{D}$ with g as $g\to 0$, schematically rewrite Eq. (38) as

$$\mathbf{D}\sim g\int \frac{\mathbf{k}}{\sqrt{1-\exp(-N_{cc}|\kappa_x|)}}[\hat{f}]_{\mp}d^2\kappa, \tag{40}$$

since $\kappa\hat{c}(\kappa)$ is order unity for most modes. The component of deflection in the ''x'' direction, D_x, may be estimated by

$$D_x\sim g\int_0^{g^2/N_{cc}} \frac{\kappa_x}{\sqrt{1-\exp(-N_{cc}|\kappa_x|)}}\,d\kappa_x + g^3\int_{g^2/N_{cc}}^{1} \frac{\kappa_x^2}{[1-\exp(-N_{cc}|\kappa_x|)]^{3/2}}\,d\kappa_x \sim g^3, \tag{41}$$

where the estimate $[\hat{f}]_{\mp}=O(1)$ was used in the first integrand $[\hat{f}]_{\mp}\sim g^2\boldsymbol{\kappa\kappa}\cdot\mathbf{M}/[1-\exp(-N_{cc}|\kappa_x|)]$ was used in the

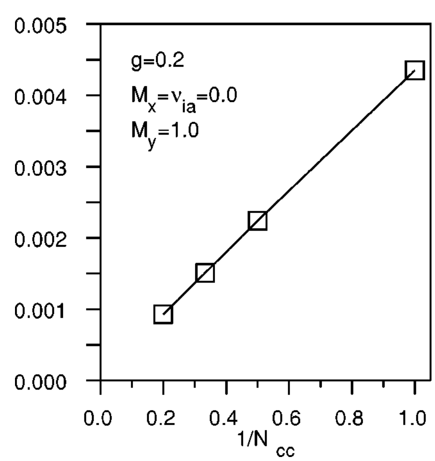

FIG. 5. Normalized y deflection rate is shown as a function of N_{cc}, for $g=0.2$, $M_x=0$ and $M_y=1.0$.

Downloaded 10 Mar 2009 to 129.105.69.71. Redistribution subject to AIP license or copyright; see http://pop.aip.org/pop/copyright.jsp

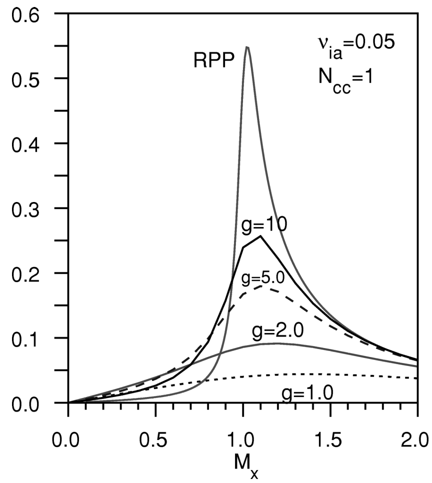

FIG. 6. Normalized x deflection rate for $M_y=0$, $\nu_{ia}=0.05$, and $N_{cc}=1$.

second. Equation (41) is dominated by large κ_x because of the factors of κ_x in the numerator. Similarly,

$$D_y \sim g \int_0^{g^2/N_{cc}} \frac{1}{\sqrt{1-\exp(-N_{cc}|\kappa_x|)}}\, d\kappa_x + g^3 \int_{g^2/N_{cc}}^{1} \frac{1}{[1-\exp(-N_{cc}|\kappa_x|)]^{3/2}}\, d\kappa_x \sim g^2/N_{cc} \tag{42}$$

and the last relation follows because both integrals are controlled by small κ_x. Deflection in the ''x'' direction apparently cannot take advantage of the relatively large correlation times available at long wavelengths (small κ_x), while deflection in the ''y'' direction can, with the result that for short correlation times, deflection along the spectrally dispersed, ''x,'' direction vanishes more quickly than in the orthogonal direction.[22] In other words, by orienting the dispersion along the direction of the flow, beam deflection is minimized.[23]

The small g limit of D_x is different than that reported in Ref. 9 because in that work the model of laser incoherence had $\hat{f}(\omega)-1 \xrightarrow[\omega\to 0]{} |\omega|$, while here this limit goes like $|\omega|^2$.

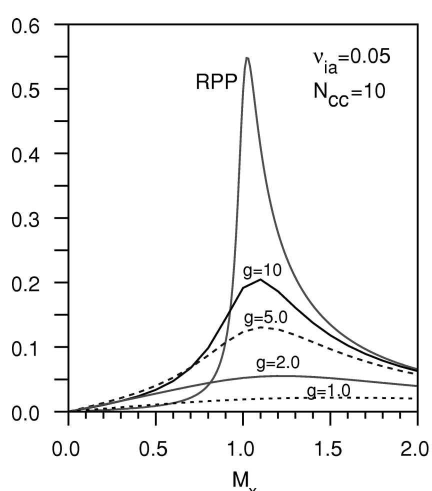

FIG. 7. Same as Fig. 6 but with $N_{cc}=10$.

A numerical study of the $g\to 0$ limit is shown in Fig. 4 for $N_{cc}=1$, with D_x evaluated for $M_y=0$ and $M_x=1.0$, and D_y evaluated for $M_x=0$ and $M_y=1.0$. Based upon the data points for $g=0.1$ and $g=0.2$, the following power law fits to the data are obtained (to two significant figures), $D_x=0.044g^{3.0}$ and $D_y=0.11g^{2.0}$, consistent with the above estimates. Inspection of the figure shows that this fit is good up to $g\approx 0.5$. These results imply that for a plasma flow not nearly aligned along either the x or y axes, the beam deflection will almost be perpendicular to the dispersive direction for small values of N_{cc}. In Fig. 5 D_y is shown as a function of N_{cc}, for $g=0.2$, $M_x=0$ and $M_y=1.0$. The numerical data is consistent with the predicted $1/N_{cc}$ behavior.

B. Finite Landau damping model

In order that the frequency integral allow for a simple evaluation for finite ν_{ia}, as a model the phase decorrelation function will now be chosen as $\exp(-\gamma|t|)$ instead of $\exp(-\gamma^2 t^2)$, and then in place of Eq. (33) one has

$$\hat{f}(k_x,\omega)=\frac{2}{\gamma(k_x)[1+(\omega/\gamma(k_x))^2]}, \tag{43}$$

and in place of Eq. (35),

$$\mathbf{D}(\mathbf{M},\nu_{ia},g,N_{cc}) = \frac{n_0}{4\pi n_c}\frac{|\langle\delta n\rangle|}{n_0}\int \frac{2}{1+\Omega^2}\frac{i\boldsymbol{\kappa}\hat{c}(\kappa)}{1-u^2-2i\nu_{ia}u}\, d\boldsymbol{\kappa}\, d\Omega. \tag{44}$$

The integral over Ω may be evaluated by residues where only the pole at $\Omega=i$ is needed,

$$\mathbf{D}(\mathbf{M},\nu_{ia},g,N_{cc})=\frac{n_0}{2n_c}\frac{|\langle\delta n\rangle|}{n_0}\int \frac{i\boldsymbol{\kappa}\hat{c}(\kappa)}{1-u^2-2i\nu_{ia}u}\, d\boldsymbol{\kappa}, \tag{45}$$

where the term ''u'' is obtained from Eq. (36) by replacing Ω by i.

In Fig. 6 the normalized deflection rate in the x direction is shown for $M_y=0$, $\nu_i=0.05$, and $N_{cc}=1$, and in Fig. 7 it is shown for $N_{cc}=10$. Increasing N_{cc} does not lead to a significant decrease in D unless g is of order unity or less because otherwise all phases are nearly static and the dynamic component of the SSD phases are nearly static phase shifts added to an already random component induced by the RPP.

VI. RELATION TO OTHER WORK

It has been observed in simulations of FM-SSD that self-focusing as well as beam deflection by flow is reduced[7,23] compared to the static RPP case. Further comparison with that work is not possible because the results of only one case were published. It is not clear to what extent the RPM-SSD and FM-SSD models considered here should have similar beam deflection properties.

The fact that the approach to ISI like behavior for beam deflection[9] is seen with only a modest number of color cycles is an important simplification since then the deflection is strictly parallel to the flow, and is a function of only three parameters, M, ν_{ia} and g, instead of a vector function of five parameters.

Downloaded 10 Mar 2009 to 129.105.69.71. Redistribution subject to AIP license or copyright; see http://pop.aip.org/pop/copyright.jsp

ACKNOWLEDGMENTS

We acknowledge valuable discussions with Joshua Rothenberg and Richard Berger, and thank them for providing preprints and unpublished notes on their SSD related research.

[1] J. Lindl, Phys. Plasmas **2**, 3933 (1995).
[2] J. D. Moody, B. J. MacGowan, D. E. Hinkel, W. L. Kruer, E. A. Williams, K. Estabrook, R. L. Berger, R. K. Kirkwood, D. S. Montgomery, and T. D. Shepard, Phys. Rev. Lett. **77**, 1294 (1996).
[3] N. D. Delamater, T. J. Murphy, A. A. Hauer, R. L. Kauffman, A. L. Richard, E. L. Lindman, G. R. Magelssen, B. H. Wilde, D. B. Harris, B. A. Failor, J. Wallace, L. V. Powers, S. M. Pollaine, L. J. Suter, R. Chrien, T. D. Shepard, H. A. Rose, E. A. Williams, M. B. Nelson, M. D. Cable, J. B. Moore, M. A. Salazar, and K. Gifford, Phys. Plasmas **3**, 2022 (1996).
[4] B. Bauer, private communication (1996).
[5] S. G. Glindinning, private communication (1996).
[6] H. A. Rose, Phys. Plasmas **3**, 1709 (1996).
[7] D. E. Hinkel, E. A. Williams, and C. H. Still, Phys. Rev. Lett. **77**, 1298 (1996).
[8] S. Ghosal and H. A. Rose, Phys. Plasmas **4**, 2376 (1997).
[9] S. Ghosal and H. A. Rose, Phys. Plasmas **4**, 4189 (1997).
[10] Y. Kato and K. Mima, Appl. Phys. B: Photophys. Laser Chem. **29**, 186 (1982).
[11] R. Lehmberg, A. Schmitt, and S. Bodner, J. Appl. Phys. **62**, 2680 (1987).
[12] S. Skupsky, R. W. Short, T. Lessler, R. S. Craxton, S. Letzring, and J. M. Soures, J. Appl. Phys. **66**, 3456 (1989).
[13] J. E. Rothenberg, D. Eimerl, M. H. Key, and S. V. Weber, Proc. SPIE **2633**, 162 (1995).
[14] D. M. Pennington, M. A. Henesian, S. N. Dixit, H. T. Powell, C. E. Thompson, and T. L. Weiland, Proc. SPIE **1870**, 175 (1993).
[15] H. Nakano, K. Tsubakimoto, N. Miyanaga, M. Nakatsuka, T. Kanabe, H. Azechi, T. Jitsuno, and S. Nakei, J. Appl. Phys. **73**, 2122 (1993).
[16] K. Tsubakimoto, M. Nakatsuka, N. Miyanaga, T. Jitsuno, T. Kanabe, H. Nakano, and S. Nakai, Proc. SPIE **1870**, 186 (1993).
[17] Fluctuations in ϵ owing to ϕ are Gaussian in this limit.
[18] While effects such as the supersonic layering instability and flow exclusion, as described in Ref. 6, are not captured by linearized hydrodynamics, for small enough average laser intensity the length scales associated with these phenomena are large compared to a speckle width so that locally, i.e., over the scale of many speckle widths, the linearized hydro response is valid.
[19] For this to be accurate, the ion pressure must be negligible.
[20] This is only superficially different in form from Eq. (10) of Ref. 9, owing to the introduction of a minus sign in our definition of a now dimensionless linear hydro response function, and the presence of a factor of 1/2 in Eq. (3) of the same reference which is absent in our definition of the correlation function, C.
[21] See Eq. (157) of Ref. 8. Because of a difference in normalization, what is plotted as the RPP deflection in this paper is actually $(128/90\pi) f(M,g_0)$, where $f(M,g_0)$ is the universal flow function defined by Eq. (116).
[22] It can be shown, however, that D_y vanishes unless the plasma flow has a finite component along the y axis.
[23] Such an ansatz was considered by Dick Berger, Bruce Langdon, Edward Williams (private communication, 1997), but no such effect was found in their simulations with FM-SSD.

Downloaded 10 Mar 2009 to 129.105.69.71. Redistribution subject to AIP license or copyright; see http://pop.aip.org/pop/copyright.jsp